Hindawi Publishing Corporation
Chinese Journal of Engineering
Volume 2014, Article ID 270527, 8 pages
http://dx.doi.org/10.1155/2014/270527

Research Article

Hybrid Effect of Nanosilicates and MWNT on Mechanical, Thermal, and Dynamic Mechanical Properties of Polypropylene

Priyanka Pandey,[1] Smita Mohanty,[1,2] and Sanjay K. Nayak[1,2]

[1] *Central Institute of Plastics Engineering and Technology (CIPET), Chennai 600 032, India*
[2] *Laboratory for Advanced Research in Polymeric Materials (LARPM), CIPET, Bhubaneswar 751024, India*

Correspondence should be addressed to Sanjay K. Nayak; papers.journal@gmail.com

Received 19 November 2013; Accepted 18 December 2013; Published 23 January 2014

Academic Editors: B.-Y. Cao and R. Hong

A two-step process was used to prepare PP/MAPP/C15A/MWNT ternary nanocomposites system. The effect of the addition of MWNT on the delamination of clay layers in the polymer matrix has been studied through XRD. The similar crystallinity level was noticed after the addition of clay and MWNT together in the PP matrix through XRD. Higher mechanical properties of the ternary nanocomposites system were noticed than neat PP and its binary nanocomposites systems. Differential scanning calorimeter (DSC) technique was utilized to investigate the effect of both nanofillers on crystallization temperature (T_C). And a shift in T_C towards higher temperature was noticed in all the nanocomposites. Thermogravimetric analysis revealed an improved thermal stability of the ternary nanocomposites system. The dynamic mechanical response of PP and its binary and ternary nanocomposite systems was evaluated. The dispersion of the nanoparticles was investigated employing transmission electron microscopy (TEM). The combined effect of clay and MWNT on the properties of PP was investigated and summarized.

1. Introduction

Polymers, reinforced with nanoscaled fillers, developed an advanced multifunctional material with improved properties which can be used in many fields ranging from microelectronics to aerospace. And because of good balance between properties and cost, low density, and easy moldability, polypropylene is the chosen material among all polymers [1]. In case of PP nanocomposites, maleic anhydride grafted PP has been proved to enhance the compatibility between PP and fillers [2].

Nanoscale fillers are also important in improving mechanical and other properties along with changes in crystallization behaviour [3]. Recently polymer layered silicate nanocomposites have attracted intense attention of industry and academicians for achieving various excellent properties including flame retarding characteristics for polymer due to its excellent barrier effect [4, 5].

Studies also have been reporting that MWNT, because of their exceptional mechanical and thermal properties, has become attractive class of inclusion [6]. The MWNT forms networked layers in polymer matrix, shielding the polymer from external radiation and flame. It also acts as excellent thermal insulation. The mechanical properties of MWNT are exciting, since they are considered as the ultimate carbon material ever made.

Combination of these two fillers nanoclay and MWNT has attracted much of the current interest owing to their extended structure allowing for clay nanolayer and carbon nanotubes network assemblies. Earlier various studies were primarily focused on dispersion of single nanofiller (clay or MWNT) into the polymer matrix, wherein various short falls have been reported. However very few literatures have reported the combined effect of MWNT and clay on single polymer matrix. It has been noticed preciously that MWNT and nanoclay exhibit synergism in improving the flame retardancy of ABS [7]. Earlier synergistic effects of MWNT and sepiolite nanoclay on the flammability of PP nanocomposites have been reported [8].

The aim of this work was to investigate the effect of incorporation of MWNT and layered silicates (MMT) based on nanoclay on the polypropylene (PP) matrix. The process

parameters of the preparation of ternary nanocomposites were optimized in order to achieve the improved mechanical properties. The morphological conditions (intercalation/exfoliation) were also investigated through XRD and TEM. The dynamic mechanical analysis of the PP and its binary and ternary nanocomposites has been performed in order to evaluate the molecular mobility transition such as glass transition. This transition represents the ability of heat resistance [9]. This study also aimed to determine crystallization behaviour and thermal stability of ternary nanocomposites, using DSC and TGA techniques, respectively.

2. Materials

Polypropylene (M110) was procured from M/s Haldia Petrochemicals, Kolkata, India, having a density of 0.94 g/cm^3 and the MFI of 11 g/10 min. The clay minerals used were commercially available Cloisite 15A (cation exchange capacity (CEC) of 125 meq/100 g clay, d_{001} of 3.15 nm), with organic modifier dimethyl, dehydrogenated tallow, quaternary ammonium (2M2HT) was purchased from M/s Southern clay products, Inc. USA, having a diameter of about 10–30 nm a length of 100 micrometers. Multiwalled carbon nanotubes of >98% purity and diameter of 80–100 nm, used in this work, were purchased from M/s Nanoshel, Intelligent Materials Pvt. Ltd, India. The MWNT used in this study was purified in the presence of HNO_3 before incorporating into PP/MAPP/C15A hybrid. The compatibilizer used in this study was PP-g-MA, (OPTIM-P425), having an anhydride content of 1.6–2.5% and density 0.91 g/cm^3, and purchased from M/s Pluss Polymers Pvt. Ltd., Haryana, India.

3. Experimental

3.1. Preparation of Nanocomposites. The masterbatch route was employed to prepare the nanocomposites using microinjection molding technique. First the PP/MAPP/C15A hybrid was synthesized with a 5 Wt% loading of MAPP and 3 Wt% loading of C15A using microcompounder, M/s DSM explore Netherlands, (Micro 15 at a temperature of 180, 185, and 185°C in front, middle, and rear zone resp. for 20 minutes as obtained from a previous study [10]). In the second step 0.3% of MWNT was mixed to the PP/MAPP/C15A hybrids at a temperature of 180°C in all zones.

In this step variable mixing time and screw speed of 60 rpm for 5 min, 30 rpm for 15 min, and 30 rpm for 22 min were used in order to optimize the process parameters as well as improved dispersion of MWNT within PP matrix. The mixing parameters have been optimized as 180°C with 30 rpm for 22 minutes, on the basis of mechanical properties.

3.2. X-Ray Diffraction Analysis (XRD). Wide angle X-ray diffraction (WAXD) analysis was used to analyze the interlayer gallery spacing of nanoclays in the nanocomposites, using Philips X'Pert MPD (Japan), with graphite monochromator and a Cu Kα radiation source operated at 40 kv and 30 mA. The X-ray radiation source having wavelength of 1.54 A0 (copper Kα_1, Ni filter), aperture slit having width 0.1 mm, and the scanning rate of 0.01 degrees per/s over the range of $20 < 2\theta < 800$ (for clay) and $20 < 2\theta < 100$ (PP and its nanocomposites) were used.

3.3. Mechanical Properties. The tensile properties of the virgin matrix as well as the nanocomposites were determined using Universal Tensile Machine (3382 Instron, UK) as per ASTM D 638. Microinjection moulded sample having dimension of $127 \times 12.7 \times 3$ mm^3 was subjected to tensile test at a gauge length of 50 mm and speed of 5 mm/min and the Izod impact strength of the samples (dimension: $63.5 \times 12.7 \times 3$ mm^3) has also been investigated using a Tinius Olsen, USA, impactometer as per ASTM D 256. The samples were notched as "V" notch depth of 2.54 mm and notch angle of 45°, prior to loading with hammer of 2 J.

3.4. Differential Scanning Calorimeter (DSC). Differential scanning calorimetry (DSC) measurement was carried out by scanning the sample about 10 mg, from −50 to 200°C with heating rate of 10°C/min under nitrogen atmosphere using Q 20 series of TA instrument.

3.5. Thermogravimetric Analysis (TGA). The thermal degradation temperatures and thermal stability of the PP and its nanocomposites were studied using a thermogravimetric analyzer (Q50 M/s TA instrument, USA). Samples of ≤10 mg were heated from 50 to 680°C at a heating rate of 10°C/min. corresponding initial, maximum, and final degradation temperature were calculated.

3.6. Dynamic Mechanical Analysis (DMA). The DMA analysis was conducted in dual cantilever mode at variable temperature using dynamic mechanical analyzer (DMA Q-800; TA instruments) technique. The experiment performed on the microinjection moulded samples having a dimension $63.5 \times 12.7 \times 3$ mm^3 was used.

3.7. Transmission Electron Microscopy (TEM). TEM analysis was of the samples carried using the transmission electron microscope (JEOL 1200EX, Japan). The thin sections have been taken from injection moulded bar, using microtome, Lieca EM UC6 microtome (M/s Leica, Germany), under cryo conditions, for analysis. The sections were collected from water on 300-mesh carbon-coated copper grids. TEM imaging was carried out at an accelerating voltage of 100 kV. Images were captured using a charged couple detector (CCD) camera for further analysis using Gatan Digital Micrograph analysis software.

4. Result and Discussion

4.1. XRD. In order to achieve high performance nanocomposites, good dispersion of the nanofiller and strong interfacial adhesion between nanofiller and the matrix are the major requirements. The microstructural configuration was examined using XRD. Figure 1 represents the XRD spectrum of PP, PP binary, and ternary nanocomposites. In the spectra of clay main peak (001) corresponding to basal

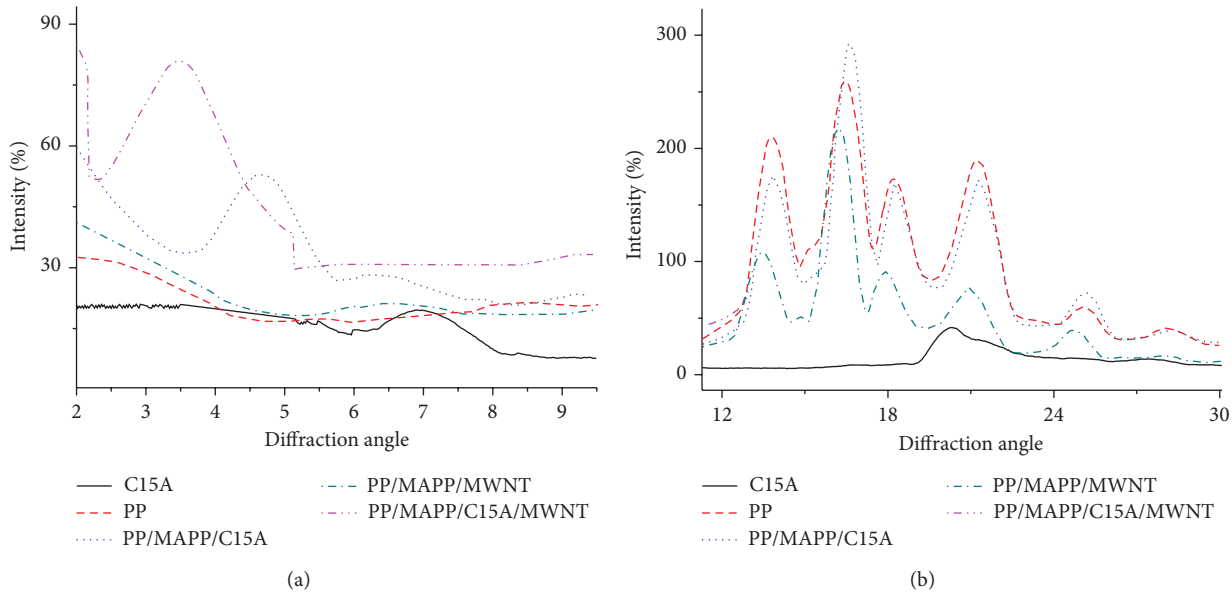

Figure 1: X-ray diffraction pattern (a) from $2\theta = 2$ to 10 and (b) $2\theta = 2$ to 80.

plane reflection was found at a diffraction angle of $2\theta = 7$, revealing the intergallery spacing of 1.13 nm. In case of PP/MAPP/C15A, the diffraction angle for 001 plane was shifted to $2\theta = 4.7$ to a corresponding intergallery spacing of 1.63 nm. This depicted the intercalation of clay layers due to the insertion of polymer macromolecular chains. Further, in the spectra of PP/MAPP/C15A/MWNT nanocomposites, the peak corresponding to 001 plane shifted to lower diffraction angle of $2\theta = 3.5$ ($d_{001} = 1.87$ nm), exhibiting the increased degree of delamination of clay layers.

4.2. Mechanical Properties. Table 1 represents tensile modulus, stress at yield, elongation at break, and impact strength for pure PP and its nanocomposites. The mechanical properties of the ternary nanocomposites at different process parameters were compared. It was noticed that mixing of MWNT in PP/MAPP/C15A hybrid at 180°C with 60 rpm for 5 min was lower than PP/MAPP/C15A hybrid. However increasing the time to 15 min also revealed the reduced properties. Further the increase in the time to 22 min with reduced rpm has provided much enhanced mechanical performance. The rpm was reduced to avoid the possible degradation during residence time while mixing. In all variations of time and rpm the temperature was constant.

Analysis revealed the higher tensile properties of PP/MAPP/C15A nanocomposites as compared to neat PP was noticed. This was due to uniform nanodispersion and intercalation of nanoclays. It is assumed that the strong hydrophilic interaction between the MA group and the polar clay surfaces has been achieved, which might be driving force of the intercalation. The tensile properties of PP/MAPP/MWNT nanocomposite were also higher than that of neat PP. This was also ascribed to the nanodispersion of clay particles inside the PP matrix leading to the even stress distribution.

Table 1: Mechanical properties of the PP and its nanocomposites.

Properties	VPP	PP/MAPP/C15A	PP/MAPP/C15A/MWNT		
			5 min 60 rpm	15 min 60 rpm	22 min 30 rpm
Impact strength (j/m)	25	22	20	22	31
Tensile stress (MPa)	30	33	32	37	41
Tensile strain (%)	8	6	6	5	8
Modulus (MPa)	1136	1454	1408	1443	1521

Further, in case of ternary nanocomposites, increase of 23.6%, 4.65, and 19.5% was noticed in tensile strength, tensile modulus, and impact strength, respectively, as compared to PP/MAPP/C15A. Similarly as compared to PP/MAPP/MWNT also, ternary nanocomposites had 15%, 3%, and 11% higher tensile strength, tensile modulus, and impact strength, respectively. This might be ascribed to the more intact 3D network achieved by clay-clay, clay-MWNT, and clay-polymer-MWNT interaction, resulting in disruption of MWNT network by the layered silicates forming islands isolated by clay platelets [11]. This provides more uniform stress distribution to the fillers.

Further, the elongation at break was found to be lower for nanocomposites. This supports the fact that increase in modulus leads to decreased mechanical ductile nature. However, it is not disadvantageous, since several applications require high stiffness of material and low deformation in order to ensure higher-dimensional stability [12].

Further, in order to strengthen the finding of the tensile data the Izod impact strength was analyzed. The analysis

Table 2: Differential scanning calorimeter results of PP and its nanocomposites.

Material	T_m (°C)	$T_{c(\text{onset})}$ (°C)	$T_{c(\text{end})}$ (°C)	T_c (°C)
PP	166	119	110	109
PP/MAPP/MWNT	167	131	109	123
PP/MAPP/C15A	169	129	107	118
PP/MAPP/C15A/MWNT	168	139	110	127

revealed the higher impact strength of the ternary nanocomposites. It is expected that the nanofillers create tie points between crystallites, bridging the amorphous phase, due to different possible interactions as mentioned earlier in this section.

4.3. Differential Scanning Calorimeter (DSC). The mechanical properties of the polymer matrix are very much dependent on the crystallinity and microstructure, since failure of material takes place at the microscopic level. The microstructural properties are directly reflected by exothermic or endothermic transition in DSC thermogram. The result obtained from DSC analysis is represented in Table 2. From the analysis no substantial difference was noticed in melting point of neat PP and its binary and ternary nanocomposites. However the crystallization temperature of the PP/MAPP/C15A/MWNT nanocomposites was found higher as compared to PP and binary nanocomposites. Higher T_C of ternary nanocomposites revealed the hybrid nucleation effect of both the fillers on the PP matrix. Further, the narrower crystallization and melting peak of the ternary nanocomposites as compared to the PP and its binary nanocomposites (PP/AMPP/C15A and PP/MAPP/MWNT) exhibited the narrower crystallite size distribution.

4.4. Thermogravimetric Analysis (TGA). The thermal stability is a unique ability to promote flame retardancy in polymer nanocomposite. The degradation temperature at different stages has been observed and reported in Table 3. The different temperatures which have been reported are $T_{d(0.1)}$: temperature for 10% weight loss, $T_{d(0.5)}$: temperature for 50% weight loss, $T_{d(0.95)}$: temperature for 95% weight loss, $T_{d(\text{onset})}$: onset temperature for degradation, $T_{d(\text{end})}$: end temperature for degradation, and $T_{d(\max)}$: peak temperature for degradation. From the data it is evident that $T_{d(0.1)}$and $T_{d(0.5)}$ are shifted towards higher temperature for nanocomposites, wherein the increase in the $T_{d(0.1)}$ as compared to virgin PP is 3°C, 7°C, and 37°C higher for PP/MAPP/C15A, PP/MAPP/MWNT, and PP/MAPP/C15A/MWNT, respectively. This might be attributed to the reinforcing effect of the nanoclay and MWNT, which results in the formation of char layer.

Further, the $T_{d(0.95)}$ of the PP/MAPP/C15A hybrid was lower as compared to the neat PP matrix, which indicated the lower stability of layered silicate and MWNT at higher temperature and therefore it also starts degrading as polymer matrix. This instability is because the alkylammonium cation in organoclay suffers decomposition following the Hoffman elimination reaction and its product in turn with itself catalyses the degradation of polymer matrix [13]. However, in case of PP/MAPP/MWNT, the reason for this decrease is not clear. In case of PP/MAPP/C15A/MWNT the $T_{d(0.95)}$ showed a shift towards a higher temperature. This is due to hybrid effect of clay and MWNT in improving thermal stability of PP.

The onset degradation temperature ($T_{d(\text{onset})}$) of PP/MAPP/C15A and PP/MAPP/MWNT was delayed and found to be respectively, 27°C and 41°C higher, as compared to neat PP. The similar pattern was observed in case of final degradation temperature ($T_{d(\text{end})}$) too. This shift might be attributed to the formation of high performance, carbonaceous char that gets build-up on the surface, in the presence of clay or MWNT, insulating the underlying material and slowing the degradation and escape of volatile products generated during decomposition. The relatively higher $T_{d(\text{onset})}$ of the PP/MAPP/MWNT as compared to PP/MAPP/C15A might be attributed to the migration of MWNT fibrils towards the surface, leading to the formation of thin but continuous shielding network covering the entire sample. However, due to a higher loading of clay as compared to MWNT, thick char layer is formed in case of PP/MAPP/C15A but its shielding is less influential due to discontinuity in the layers [14].

However, more delayed degradation in case of ternary nanocomposites was noticed. An increase of 82°C in the onset degradation temperature was evident. This was relatively higher as compared to its binary counterparts (i.e., PP/MAPP/C15A and PP/MAPP/MWNT). This suggests the presence of porous char layer with microcracks in PP/MAPP/C15A, whereas the PP/MAPP/MWNT is supposed to have continuous char layer with less density. The highly delayed degradation of ternary nanocomposites is ascribed to relatively tighter and denser char. This can be attributed to two types of mechanism. Some MWNTs act as the bridge and overlap the pores between clay layers, and the remaining MWNTs get inserted between clay layers and form a sandwich structure leading to intercalation of clay layers [7].

Also the decomposition of nanocomposites was found sharper than PP, pertaining to a reduced range of decomposition for nanocomposites as compared with virgin PP. This supports the fact that the addition of nanofiller improves the uniformity of the crystalline structure of the polymer matrix. Hence, in ternary nanocomposites more uniformity of crystalline structure was evident from sharper degradation peak. This may also be attributed to the restricted thermal motion of polymer and MWNT in the intergallery of clay platelets. These results were in accordance with the findings reported earlier [15]. Further, the peak decomposition temperatures ($T_{d(\max)}$) of binary nanocomposites were found lower as compared to the neat PP matrix. This might be due to the conduction of heat due to intercalated structure [16]. However higher $T_{d(\max)}$ of PP/MAPP/MWNT as compared to neat PP revealed the reinforcing effect of MWNT fibrils inside the PP matrix, whereas the $T_{d(\max)}$ of PP/MAPP/C15A/MWNT was higher than that of PP and PP/MAPP/C15A hybrid. This supports the fact that exfoliated morphology may be achieved

Table 3: Thermogravimetric analysis of PP and its nanocomposites.

Composition	$T_{0.1}$ (°C)	$T_{0.5}$ (°C)	$T_{0.95}$ (°C)	$T_{d(\text{onset})}$ (°C)	$T_{d(\text{end})}$ (°C)	$T_{d(\text{max})}$ (°C)
PP	384	430	450	319	440	440
PP/MAPP/C15A	387	431	433	360	441	429
PP/MAPP/MWNT	391	438	445	326	476	445
PP/MAPP/C15A/MWNT	421	445	452	401	491	458

by insertion of MWNT inside clay galleries, which in turn may cause reduced conduction of heat [16].

Therefore, it is evident that, in order to increase the overall thermal stability of polymer matrix, a high degree of exfoliation accompanied with fine dispersion is required. In this study this exfoliation was achieved with the incorporation of MWNT in PP/MAPP/C15A hybrids, which in turn resulted in improved thermal stability.

Hence it may be concluded that plate like particles of high aspect ratio are not the only filler suitable for thermal improvement. Independent of aspect ratio nanoparticles with high specific area are also suitable entity for improving thermal stability, by absorbing radicals and high polar groups. This mechanism involves the physical/chemical adsorption of volatile degradation product on particle surface. This imparts more thermal stabilization in the polymeric system [11].

4.5. Dynamic Mechanical Analysis (DMA). In order to interpret the unique property variation of PP and its nanocomposites, including melt fluidity, crystallization habit, and thermal stability as well as storage modulus, the role of the addition of nanofillers on the mobility of PP chains needs to be identified. The storage modulus is related to the stiffness of the material and measures the elastic response of the polymer. The loss modulus denotes the energy dissipated by the system in the form of heat and measures the viscous response of the polymer material. The damping factor (tan δ) is a ratio of loss modulus to storage modulus. In PP over the entire temperature range, two main mechanical relaxation processes were evident, namely, high temp α relaxation, related to the crystalline fraction present, and a β process, related to the glass rubber transition relaxation.

The dynamic storage modulus is shown in Figure 2(a) as a function of temperature. General falling trend was observed for all the cases. The higher initial value of storage modulus was observed for each sample at a subambient temperature. This supports the fact that molecules remain in frozen state at this condition; hence, they show high stiffness properties in glassy condition. A clear transition was observed at 0°C. This transition might be related to the glass (β) transition. For all the cases, it was found that the storage modulus value decreases with the increase in temperature, below glass transition temperature. This might be due to the fact that PP reaches its softening point and therefore reduces the elastic response of the material. A considerable drop was noticed in the vicinity of glass transition temperature. Indicating the phase transition from the rigid glassy state where the molecular motions are restricted to a more flexible rubbery state and the molecular chains have more freedom to move. Furthermore, with increase of temperature to the melting temperature the storage modulus of nanocomposites is dominated by matrix intrinsic modulus.

Furthermore, it was noticed that the storage modulus of nanoclay and MWNT reinforced binary nanocomposites was higher as compared to the neat PP. This confirmed the uniformly distributed stress over the nanoclay and MWNT in their individual nanocomposites. Subsequently, higher storage modulus of ternary (PP/MAPP/C15A/MWNT) nanocomposites as compared to the its binary counterparts exhibited more intact percolated network in PP/MAPP/C15A/MWNT than in PP/MAPP/C15A and PP/MAPP/MWNT. Hence it is evident that coexistence of clay and MWNT in the polymer matrix creates more effective confined space and enhances the networked structure, leading to the relatively more even distribution of the stress.

It was also observed that the curves tend to converge to that of pure PP when approaching the melting temperature of PP. This convergence at higher temperature reveals the successful exploitation of nanofillers as reinforcement for PP.

The loss modulus curve of PP, as represented in Figure 2(b), exhibited two relaxations localized in the vicinity of 89°C and 71°C. This is related to the local motions of amorphous phase, which is in turn related to the glass transition and relaxation of crystalline fraction, respectively. In nanocomposites also two relaxations were discernible. In all the nanocomposites the peak corresponding to the glass transition remains at about the same temperature as of neat PP, but with lower intensity. This suggests the equal level of crystallinity in the PP, PP/MAPP/C15A, PP/MAPP/MWNT, and PP/MAPP/C15A/MWNT nanocomposites. This was in accordance with the DSC analysis. This supports the fact that inclusion of nanofillers did not exhibit any effect on relaxation behaviour of PP. The relaxation transition peak around −3 to 7°C is expected to be related to the complex multirelaxation process, which is mainly concerned with molecular motion of the crystalline region of PP. However, higher loss modulus of ternary nanocomposites, as compared to neat PP and its individual counter parts (PP/MAPP/C15A and PP/MAPP/MWNT), suggests the high degree of mechanical interlocking between filler and bulk chains in ternary nanocomposites. This interaction can be effective in transmitting stress between the matrix and the filler. This finding was in accordance with the storage modulus analysis. Further, like storage modulus when approaching the melting temperature of PP the curves tend to converge and exhibit the intrinsic properties of PP matrix.

The damping in polymeric materials is sensitive of segmental mobility of the polymer chain and in nanocomposites

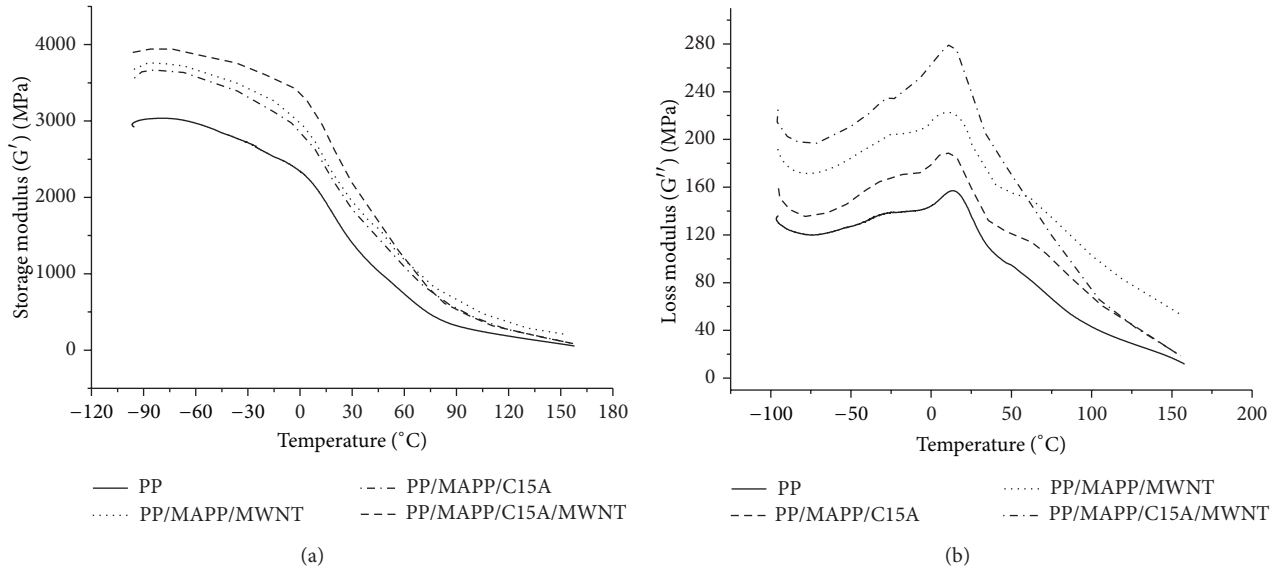

Figure 2: Dynamic mechanical properties of PP and its nanocomposites: (a) storage modulus and (b) loss modulus.

it is indicative of the interfacial interaction between the polymer and the filler. Strong interfacial interaction between the polymer and the filler tends to restrict the polymer mobility thereby reducing the damping. The damping factor of PP/MAPP/C15A was found lower than that of neat PP indicating the appropriate interaction between macromolecular polymeric chains and fillers (clay or MWNT). However it could be noticed that damping of PP/MAPPMWNT nanocomposites was higher as compared to PP/MAPP/C15A. This is because the low loading of MWNT could be dispersed uniformly in matrix but the formation of MWNT network could not take place [17].

Subsequently, a significant decrease in the damping of the ternary nanocomposites was noticed, revealing the much enhanced interaction between matrix and both the fillers together, as compared to their binary counterparts. These interactions may be in various forms as clay-clay network, clay-MWNT network, MWNT-polymer-clay bridging, and polymer-polymer network. In the clay-MWNT network clay platelets impede the motion of MWNT in polymer matrix during deformation, leading to the enhanced interaction between polymer chain and fillers, which might have played a major role in reducing the damping of ternary nanocomposites. Hence the synergistic effect of the clay and MWNT was evident.

From Figure 3, it was depicted that Tan $\delta < 1$, and this exhibited the solid like elastic behaviour of all the material at whole temperature range [18]. Further, from damping factor curve, T_g of the nanocomposites can be determined by Tan δ peak temperature. From the figure, the formation of T_g peaks in the range of −7 to 15°C was clearly observed. This was supposed to be associated with the β-relaxation of unrestricted amorphous phase in PP. This is a secondary relaxation due to movement of short chain segment. However, no significant shift was observed in T_g for PP nanocomposites. This suggested that there is no change

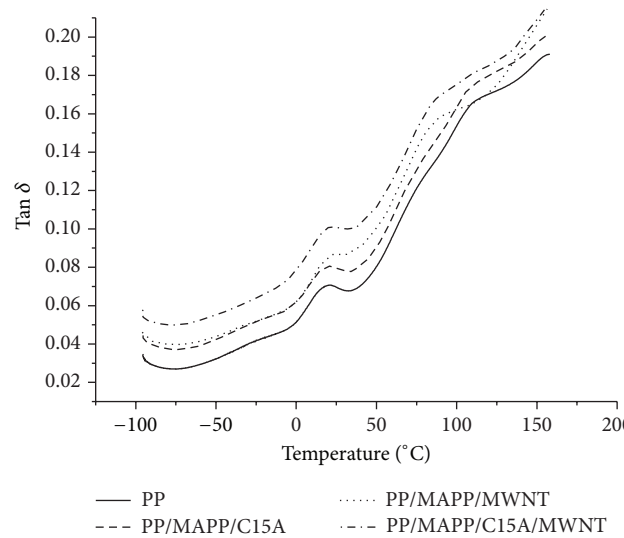

Figure 3: Tan δ versus temperature, of PP and its nanocomposites.

in the rigidity of the filler matrix interfacial zone as well as maintained even after addition the of MWNT as secondary nanoparticles.

4.6. Transmission Electron Microscopy (TEM). The TEM micrographs of PP/MAPP/C15A, PP/MAPP/MWNT, and PP/MAPP/C15A/MWNT are depicted in Figure 4. The clay particles in the micrographs are indicated by dark areas and the gray region represents the continuous PP matrix. Fine and homogenous dispersion of the clay TEM micrographs of the PP/MAPP/C15A nanocomposites revealed the mixed morphology of intercalated and exfoliated clay galleries. Also there was evidence of small aggregates of clay particles within the intercalated clay structures. However, in case of

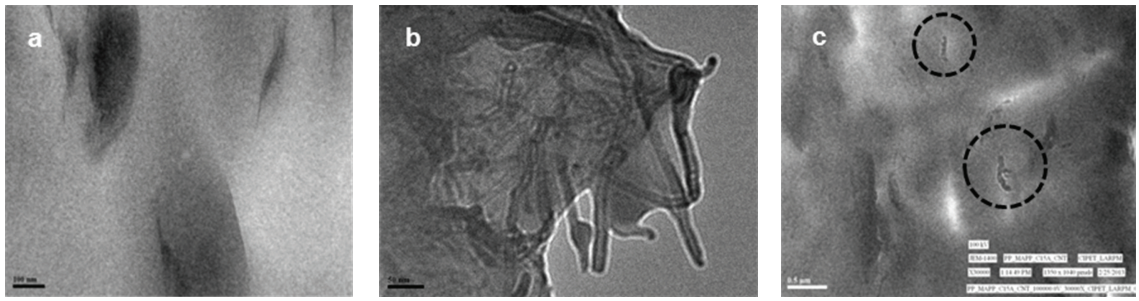

(a) (b) (c)

Figure 4: TEM micrographs of (a) PP/MAPP/C15A, (b) PP/MAPP/MWNT, and (c) PP/MAPP/C15A/MWNT.

PP/MAPP/MWNT bundled MWNT fibrils were evident, revealing the fact that the utilization of intrinsic properties of MWNT has not been carried out completely.

On the contrary, incorporation of MWNT as secondary filler in, PP/MAPP/C15A nanocomposite revealed uniform dispersion of the MWNTs and clay layers within the PP matrix as compared to the PP/MAPP/C15A nanocomposites. Higher degree of exfoliation was observed in PP/MAPP/C15A/MWNT nanocomposites. This might be due to the insertion of MWNT within the clay layers which might have resulted in the delamination of the clay layers.

The entanglement of MWNT and clay layers is evident from the micrographs, which is marked in Figure 4(c). Further the agglomerates observed in the PP/MAPP/C15A nanocomposites were absent in PP/MAPP/C15A/MWNT hybrids. This phenomenon is attributed to the improved interaction of MWNT and clay layers which facilitated the separation of stacks from each other thereby resulting in homogenous distribution within matrix polymer.

5. Conclusion

The present study revealed that the melt intercalated nanocomposite hybrids from PP clay and MWNT in the presence of compatibilizer can be obtained at relatively low screw speed and high residence time. Morphological investigation through XRD revealed much enhanced d-spacing of clay layers in ternary nanocomposites, revealing the exfoliated morphology. Incorporation of nanoclay within the PP matrix in the presence of compatibilizer results in improvement of tensile properties with no considerable improvement in the impact properties of the matrix polymer. On the contrary the addition of MWNT within the PP/MAPP/C15A nanocomposite hybrid resulted in significantly improved mechanical performance. The thermal stability of the nanocomposites increased phenomenally with the addition of MWNT, thus revealing the synergistic effect of MWNT. The dynamic mechanical analysis revealed the higher modulus in binary nanocomposites which was further higher in case of ternary nanocomposites. TEM micrographs revealed higher degree of exfoliation in the presence of both types of nanofillers (C15A and MWNT) as compared with that of C15A individually.

Conflict of Interests

The authors declare that there is no conflict of interests regarding the publication of this paper.

References

[1] E. Logakis, E. Pollatos, C. Pandis et al., "Structure-property relationships in isotactic polypropylene/multi-walled carbon nanotubes nanocomposites," *Composites Science and Technology*, vol. 70, no. 2, pp. 328–335, 2010.

[2] S. Y. Lee and S. J. Kim, "Delamination behavior of silicate layers by adsorption of cationic surfactants," *Journal of Colloid and Interface Science*, vol. 248, no. 2, pp. 231–238, 2002.

[3] C. O. Rohlmann, M. D. Failla, and L. M. Quinzani, "Linear viscoelasticity and structure of polypropylene-montmorillonite nanocomposites," *Polymer*, vol. 47, no. 22, pp. 7795–7804, 2006.

[4] J. K. Pandey, K. Raghunatha Reddy, A. Pratheep Kumar, and R. P. Singh, "An overview on the degradability of polymer nanocomposites," *Polymer Degradation and Stability*, vol. 88, no. 2, pp. 234–250, 2005.

[5] E. P. Giannelis, "Polymer layered silicate nanocomposites," *Advanced Materials*, vol. 8, no. 1, pp. 29–35, 1996.

[6] Z. Zhou, S. Wang, L. Lu, Y. Zhang, and Y. Zhang, "Isothermal crystallization kinetics of polypropylene with silane functionalized multi-walled carbon nanotubes," *Journal of Polymer Science B*, vol. 45, no. 13, pp. 1616–1624, 2007.

[7] H. Ma, L. Tong, Z. Xu, and Z. Fang, "Synergistic effect of carbon nanotube and clay for improving the flame retardancy of ABS resin," *Nanotechnology*, vol. 18, no. 37, Article ID 375602, 2007.

[8] T. D. Hapuarachchi, T. Peijs, and E. Bilotti, "Thermal degradation and flammability behavior of polypropylene/clay/carbon nanotube composite systems," *Polymers for Advanced Technologies*, vol. 24, no. 3, pp. 331–338, 2013.

[9] S. Yang, J. Taha-Tijerina, V. Serrato-Diaz, K. Hernandez, and K. Lozano, "Dynamic mechanical and thermal analysis of aligned vapor grown carbon nanofiber reinforced polyethylene," *Composites Part B: Engineering*, vol. 38, no. 2, pp. 228–235, 2007.

[10] S. K. Samal, S. Mohanty, and S. K. Nayak, "Banana/glass fiber-reinforced polypropylene hybrid composites: Fabrication and performance evaluation," *Polymer-Plastics Technology and Engineering*, vol. 48, no. 4, pp. 397–414, 2009.

[11] H. plaza, B. Reznik, M. Wilhelm, O. Arias, and A. Vargas, "Electrical, thermal, and mechanical characterization of

poly(propylene)/carbon nanotube/clay hybrid composite material," *Macromolecular Material Engineering*, vol. 297, pp. 474–480, 2012.

[12] A. M. Mazrouaa, "Chapter 14: polypropylene nanocomposites," in *Polypropylene*, InTech, San Diego, Calif, USA, 2012.

[13] R. Rezanavaz and M. K. R. Aghjeh, "Relationship between the morphology and physico-mechanical properties of polyethylene/clay nanocomposites," *IOP Conference Series: Materials Science and Engineering*, vol. 40, Article ID 012047, 2012.

[14] N. A. Isitman and C. Kaynak, "Nanoclay and carbon nanotubes as potential synergists of an organophosphorus flame-retardant in poly(methyl methacrylate)," *Polymer Degradation and Stability*, vol. 95, no. 9, pp. 1523–1532, 2010.

[15] K. Chrissopoulou, I. Altintzi, I. Andrianaki et al., "Understanding and controlling the structure of polypropylene/layered silicate nanocomposites," *Journal of Polymer Science B*, vol. 46, no. 24, pp. 2683–2695, 2008.

[16] P. Pandey, S. Anbudayanidhi, S. Mohanty, and S. K. Nayak, "Flammability and thermal characterization of PMMA/clay nanocomposites and thermal kinetics analysis," *Polymer Composites*, vol. 33, no. 11, pp. 2058–2071, 2012.

[17] V. Mittal, *Polymer Carbon Nanotubes Nanocomposites, Synthesis, Properties and Applications*, BASF SE, Polymer Research, Wiley, Ludwigshafen, Germany, 2010.

[18] A. R. Jeefferie, M. Y. Yuhazri, O. Nooririnah, M. M. H. H. Sihombing, M. A. M. Salleh, and N. A. Ibrahim, "Thermonechanical and morphological interrelationship of polypropylene-mutiwalled carbon nanotubes (PP/MWCNTs) nanocomposites," *International Journal of Basic & Applied Sciences*, vol. 10, no. 4, pp. 22–27, 2010.